any added salt (Fig. 4B), and for PS(240)-*b*-PEO(45) with 1.6 mM KF ($R = 0.10$). In the PS-*b*-PAA system, the thicknesses of both the inside and outside walls of the aggregates are uniform and equal. Their structure bears some resemblance to that of aggregated soap bubbles, and their outer surface must be hydrophilic because of the presence of the short PAA chains. The LCVs are irregular in shape in Fig. 1D but are more nearly spherical in Fig. 4. These differences may be due to the polydispersity of the primary vesicles and the softness of the wall, as well as the surface energy and the shear conditions under which the LCVs were formed. The LCVs are subject to settling due to gravity but are stable and do not coalesce at room temperature. They can also be resuspended after settling. This aggregation process may provide an easy way to trap chemicals or drugs and then isolate them from the solution.

The self-assembly of vesicles has become a topic of current interest (*7*). Chemical species (that is, bisphospholipids) were incorporated into the vesicle walls to aid aggregation of these species into higher order (multivesicular) structures. As shown here, LCVs can be formed spontaneously under various conditions. They are thus a normal aggregate morphology. These higher order structures might be of interest in the development of methods for processing artificial tissuelike composites and soft biomaterials (*7*). In addition, the application of these structures in controlled drug delivery is a distinct possibility because the multiple concentric layers could provide a convenient timing mechanism.

The aggregate morphology of small-molecule amphiphiles can be changed by added salt (*8*), but much higher salt concentrations are needed (usually $\geq 10^{-1}$ M) compared with those in the present system (10^{-4} M for $CaCl_2$ or 10^{-2} M for NaCl). Changing the salt or acid content has a parallel effect on the morphology, as does changing the copolymer composition (*2*, *3*). Thus, the morphological changes appear to be a result of a gradual decrease in repulsion among the corona chains as the concentration of added ions increases. Both steric and electrostatic repulsions are involved among the partially ionized PAA chains (*9*). The addition of the strong acid, HCl, protonates the ionized carboxylic acid groups and shifts the PAA to a lower degree of ionization; as a result, the overall repulsion among the PAA chains is decreased.

At the onset of the morphological transition from spheres to vesicles for PS(410)-*b*-PAA(25), the $CaCl_2$ concentration is equivalent to 2.3 Ca^{2+} per 100 acrylic acid repeat units; thus, two PAA blocks share one Ca^{2+} if all the added Ca^{2+} is near the PAA chains. When the aggregates are LCVs, the number of Ca^{2+} ions per PAA block is about 1.5. Thus, the morphogenic effect is believed to be due to Ca^{2+} binding to the carboxylic acid of the PAA. Both inter- and intramolecular bridging appears possible. As a result, the effective distance between the PAA blocks is greatly reduced, which has the same effect on the morphology as does a decrease in block length. The relatively weaker morphogenic effect of added NaCl can be ascribed to both weak Na^+ binding and a screened electrostatic field of the charged PAA segments. The morphological changes in PS-*b*-PEO are also most likely caused by ion binding to the PEO blocks.

REFERENCES AND NOTES

1. C. Price, in *Developments in Block Copolymers*, I. Goodman, Ed. (Applied Science, London, 1982), vol. 1, pp. 39–80; J. Selb and Y. Gallot, *ibid.*, I. Goodman, Ed. (Applied Science, London, 1985), vol. 2, pp. 27–96; Z. Tuzar and P. Kratochvil, in *Surface and Colloid Science*, E. Matijevic, Ed. (Plenum, New York, 1993), vol. 15, pp. 1–83; M. D. Whitmore and J. Noolandi, *Macromolecules* **18**, 657 (1985); A. Halperin, *ibid.* **20**, 2943 (1987); R. Nagarajan and K. Ganesh, *J. Chem. Phys.* **90**, 5843 (1989); R. Hilfiker, D. Q. Wu, B. Chu, *J. Colloid Interface Sci.* **135**, 573 (1990); A. P. Gast, P. K. Vinson, K. A. Cogan-Farinas, *Macromolecules* **26**, 1774 (1993); I. Astafieva, X. F. Zhong, A. Eisenberg, *ibid.*, p. 7339; A. Qin, M. Tian, C. Ramireddy, S. E. Webber, P. Munk, *ibid.* **27**, 120 (1994); M. Antonietti, S. Heinz, M. Schmidt, C. Rosenauer, *ibid.*, p. 3276; O. Glatter, G. Scherf, K. Schillén, W. Brown, *ibid.*, p. 6046; L. Zhang, R. J. Barlow, A. Eisenberg, *ibid.* **28**, 6055 (1995).
2. L. Zhang and A. Eisenberg, *Science* **268**, 1728 (1995).
3. ———, *J. Am. Chem. Soc.* **118**, 3168 (1996).
4. K. Yu and A. Eisenberg, unpublished results.
5. A. Phillips EM410 microscope was used for the TEM studies. Samples were deposited from aqueous solutions onto copper EM grids that had been precoated with a thin film of polyvinyl formaldehyde plastic (Formvar) and then coated with carbon; the grids were then shadowed with a palladium-platinum alloy. A detailed description of the experimental conditions can be found elsewhere (*3*).
6. H. Shen and A. Eisenberg, unpublished results.
7. S. Chiruvolu *et al.*, *Science* **264**, 1753 (1994).
8. S. Ozeki and S. Ikeda, *J. Colloid Interface Sci.* **87**, 424 (1982); Y. Talmon, D. F. Evans, B. W. Ninham, *Science* **221**, 1047 (1983); D. D. Miller, D. F. Evans, G. G. Warr, J. R. Belare, B. W. Ninham, *J. Colloid Interface Sci.* **116**, 598 (1987); F. J. Schepers, W. K. Toet, J. C. van de Pas, *Langmuir* **9**, 956 (1993); B. J. Ravoo and J.B.F.N. Engberts, *ibid.* **10**, 1735 (1994); A. Sein and J.B.F.N. Engberts, *ibid.* **11**, 455 (1995); S. Miyagishi, H. Kurimoto, T. Asakawa, *ibid.*, p. 2951; L. L. Brasher, K. L. Herrington, E. W. Kaler, *ibid.*, p. 4267.
9. L. Zhang and A. Eisenberg, unpublished results.

10. We thank H. Shen for his consent to report results of preliminary experiments with the PS-*b*-P4VP.Mel system and C. J. Clarke, M. Moffitt, and L. Cuccia for useful discussions. We also thank the Natural Science and Engineering Research Council of Canada (NSERC) for continuing support of this research.

6 March 1996; accepted 25 April 1996

Patch-Clamp Detection of Neurotransmitters in Capillary Electrophoresis

Owe Orwar, Kent Jardemark, Ingemar Jacobson,* Alexander Moscho, Harvey A. Fishman, Richard H. Scheller, Richard N. Zare†

Gamma-aminobutyrate acid, L-glutamate, and *N*-methyl-D-aspartate were separated by capillary electrophoresis and detected by the use of whole-cell and outside-out patch-clamp techniques on freshly dissociated rat olfactory interneurons. These neuroactive compounds could be identified from their electrophoretic migration times, unitary channel conductances, and power spectra that yielded corner frequencies and mean single-channel conductances characteristic for each of the different agonist-receptor interactions. This technique has the sensitivity to observe the opening of a single ion channel for agonists separated by capillary electrophoresis.

We describe here a general method for the separation and detection of compounds that trigger the opening of ligand-gated ion channels. In addition to detecting established neurotransmitters and hormones, this method can be helpful for discovering bioactive substances and for identifying excitotoxins that promote receptor-mediated neurotoxicity. We applied this method to identify, from a three-component mixture, γ-aminobutyrate acid (GABA) and Glu, the major inhibitory and excitatory neurotransmitters in the mammalian brain (*1*, *2*), and *N*-methyl-D-aspartate (NMDA), a synthetic model agonist for NMDA receptors (*3*). Like many biologically active compounds, these compounds are difficult to

O. Orwar, A. Moscho, H. A. Fishman, R. N. Zare, Department of Chemistry, Stanford University, Stanford, CA 94305, USA.
K. Jardemark and I. Jacobson, Department of Anatomy and Cell Biology, Göteborg University, S-413 90, Göteborg, Sweden.
R. H. Scheller, Department of Molecular and Cellular Physiology, Howard Hughes Institute, Stanford University, Stanford, CA 94305, USA.
*Present address: Astra Hässle AB, S-431 83 Mölndal, Sweden.
†To whom correspondence should be addressed.

detect in physiologic samples at low concentrations because they lack strong absorption features at wavelengths longer than the water cutoff, and they are electrochemically inactive at potentials useful for the analysis of biological samples.

To improve the detection sensitivity for neurotransmitter amino acids, researchers have labeled them with highly fluorescent molecules and have quantitated them after a chemical separation. For many applications, derivatization of amino acids at low concentrations is not possible. Also, labeling is extremely difficult in water-based solution for N-blocked neuroactive amino acids and dipeptides such as NMDA, *N*-acetyl-L-aspartate, and *N*-acetyl-L-aspartyl-L-glutamate, as well as for carboxylate-substituted heterocyclics, such as quinolinate, and kynurenate. Other disadvantages of derivatization include a lack of selectivity, loss of sample integrity, and extraneous dilution of the original sample. Furthermore, traditional detection schemes for chemical separations such as fluorescence, absorbance, electrochemistry, mass spectrometry, and nuclear magnetic resonance cannot be used to determine the biological activity of separated components.

Biosensors overcome many of these challenges by identifying analytes on the basis of their biological activity, often with high sensitivity through biochemical amplification steps such as G protein (guanine nucleotide–binding protein) cascades or opening of ion channels (*4*–*6*). Patch-clamp techniques are especially promising for the detection of neurotransmitters because of their (i) high sensitivity, in which unitary ion channel currents elicited by one or a few ligand molecules can be resolved, and (ii) high selectivity, in which different receptor–ion channel complexes display characteristic conductance states, open and shut times, and other features (*5*–*7*). Patch-clamp–based biosensors have thus far been used only for in situ detection of neurotransmitters (detection of the analyte at the site of sample origin) (*5*, *6*). When receptors that can be activated by multiple endogenous ligands, such as the NMDA type of glutamate receptor, are used for in situ patch-clamp detection to study, for example, the release of excitatory amino acids (*6*), limited information about the chemical identity of agonists is obtained in complex mixtures (*8*), and an additional dimension for agonist identification is needed.

Shear *et al.* and Fishman *et al.* recently coupled single-cell biosensors with capillary electrophoresis (CE) separations in which receptor agonists were identified on the basis of their electrophoretic migration times and their biological activities (*9*, *10*). We now report a refinement of this concept by implementing patch-clamp detection in CE, which provides detailed microscopic information about the activated receptor–ion channels, including kinetics, conductance states, and open and closed times. By coupling this information with the electrophoretic mobility of the analyte, the result is a multidimensional format for agonist identification.

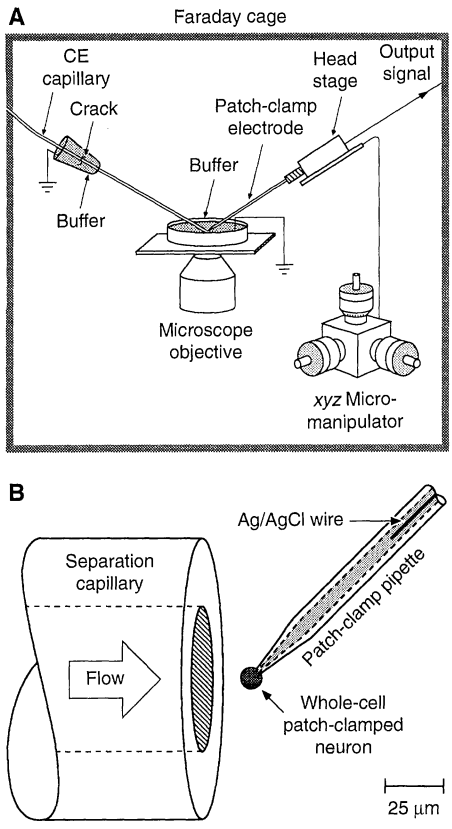

Fig. 1. Patch-clamp detection system for CE. (**A**) The inlet end (sample injection end) of a fused-silica CE separation capillary is connected to a positive high-voltage power supply through a buffer vial housed in a polycarbonate holder equipped with a safety interlock to prevent electric shock. The capillary is grounded ~5 cm above the outlet, which is positioned in the cell bath. The same buffer used for the cell bath media is used as the electrolyte in the CE capillary and inlet vial, to avoid liquid junction potentials. The tip of the patch-clamp electrode was positioned ~5 to 25 μm from the capillary outlet by means of a micromanipulator. (**B**) Schematic showing the approximate geometrical relation of the patch-clamp pipette (here depicted in the whole-cell configuration) relative to the CE separation column outlet.

We used mammalian neurons freshly dissociated from the rat olfactory bulb (*11*) as biosensors. These cells are known to have $GABA_A$ receptors (*12*) and two types of glutamate receptors: the (*R*,*S*)-α-amino-3-hydroxy-5-methyl-4-isoxazolepropionate (AMPA) and NMDA types (*11*). To obtain NMDA responses, the cells were kept in a Mg^{2+}-free, Gly-supplemented (10 μM) Hepes-saline solution (140 mM NaCl, 5 mM KCl, 1 mM $CaCl_2$, 10 mM Hepes, 10 mM glucose, pH adjusted to 7.4 with NaOH). This buffer was used as the electrolyte in the CE separations (*13*), except that Gly was left out to avoid activation of Gly-gated ion channels. For detection we used a standard patch-clamp setup (*14*) (Fig. 1A) with the tip of the patch-clamp electrode positioned 5 to 25 μm from the outlet of a fused-silica CE separation capillary (50 μm in inner diameter) (Fig. 1B). The exact positioning of the tip of the patch-clamp electrode relative to the CE capillary outlet was not critical with the analyte concentrations used. The cells were held at a membrane potential of −70 mV. Because CE is carried out at high voltages, 10 to 30 kV, and produces electric field strengths of several hundred volts per centimeter, the CE capillary was fractured and grounded ~7 cm above the outlet to create a field-free region at the position of the patch-clamp pipette tip (*13*). This procedure has been shown to be successful for high-sensitivity electrochemical detection with carbon fiber electrodes (*15*) and for two-electrode voltage clamp recordings (*9*).

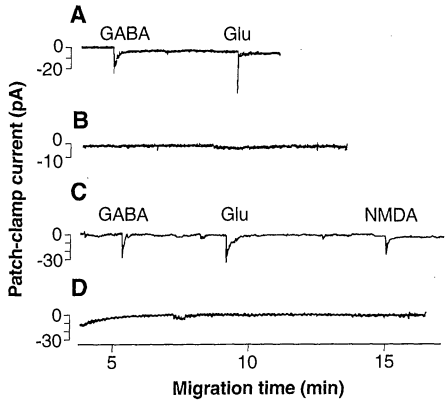

Fig. 2. Inward currents recorded from outside-out, patch-clamped olfactory interneurons after separation of GABA, Glu, and NMDA by capillary electrophoresis. (**A**) Separation of GABA (250 μM) and Glu (250 μM). (**B**) Separation of a Hepes-saline solution onto the same patch used in (A). (**C**) Separation of GABA (250 μM), Glu (250 μM), and NMDA (250 μM). (**D**) Separation of a Hepes-saline solution. Current traces were sampled at 2 Hz to display whole separations. The CE conditions (*13*) were the same for the separations, except that two different CE capillaries were used for the two respective separations and their controls.

In Fig. 2, A and C, mixed standards of GABA and Glu, and GABA, Glu, and NMDA, respectively, were separated and detected with outside-out patch-clamp detection. Electropherograms of Hepes-saline controls are shown in Fig. 2, B and D. The success rates for obtaining a receptor response from separated agonists with whole-cell and outside-out patch-clamp detection configurations were ~80% (n = 10), ~60% (n = 10), and ~90% (n = 10) for

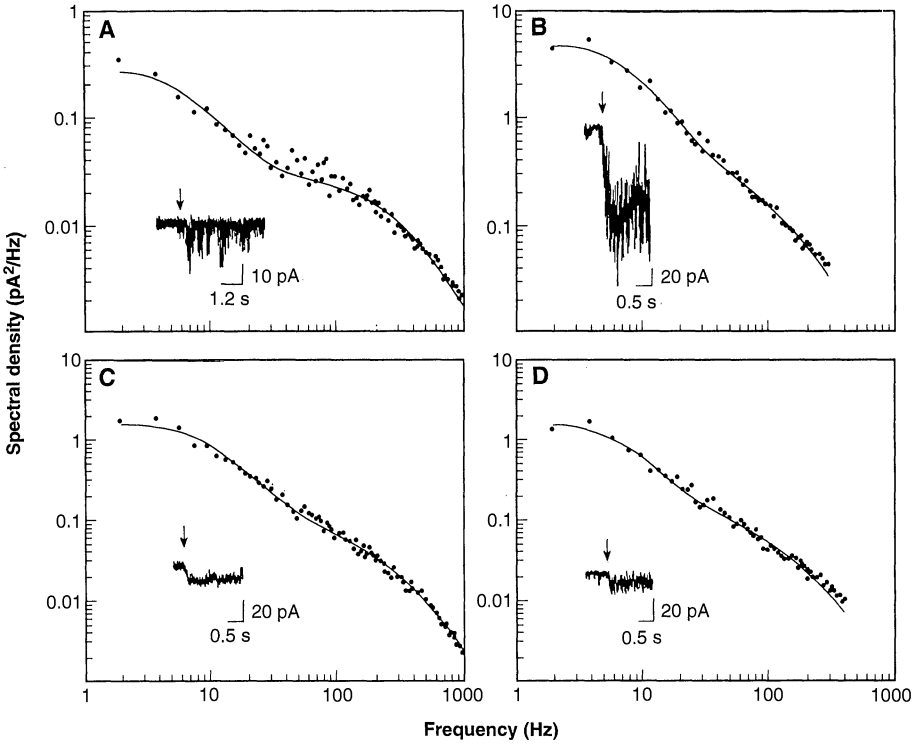

Fig. 3. Spectral analyses of whole-cell, patch-clamp current fluctuations induced by separated excitatory and inhibitory amino acids on freshly dissociated rat olfactory interneurons. Mean single-channel conductances (γ, mean ± SEM) and corner frequencies (f_{c1} and f_{c2}, mean ± SEM) were estimated from the fitted power spectra (*17*). (**A**) Power spectrum of currents elicited by GABA (250 μM) on $GABA_A$ receptors. Spectral analysis yielded γ = 22.4 ± 3.1 pS, f_{c1} = 10.1 ± 0.8 Hz, and f_{c2} = 214.2 ± 37.5 Hz (n = 6). (**B**) Power spectrum of NMDA and AMPA receptor currents evoked by Glu (250 μM). Spectral analysis yielded γ = 39.2 ± 3.0 pS, f_{c1} = 9.8 ± 0.7 Hz, and f_{c2} = 151.5 ± 39.2 Hz (n = 8). (**C**) Power spectrum of Glu-activated (250 μM) AMPA receptors (Mg^{2+} was included in Gly-free media to inhibit NMDA responses). Spectral analysis yielded γ = 10.3 ± 2.3 pS, f_{c1} = 7.0 ± 2.1 Hz, and f_{c2} = 147.7 ± 42.1 Hz (n = 3). (**D**) Power spectrum of NMDA-activated (10 μM) NMDA receptors. Spectral analysis yielded γ = 33.4 ± 4.2 pS, f_{c1} = 7.0 ± 0.4 Hz, and f_{c2} = 103.0 ± 7.2 Hz (n = 3). The insets show examples of whole-cell currents elicited by the respective receptor agonists, whose onset is indicated by the arrows.

GABA, NMDA, and Glu, respectively. The response to GABA (100 to 250 μM) was completely blocked by picrotoxin (300 μM, n = 7), the response to Glu (10 to 250 μM) in a Mg^{2+}-supplemented (1 mM) Gly-free media was completely blocked by the AMPA receptor antagonist 6-cyano-7-nitroquinoxaline-2,3-dione (CNQX, 20 μM, n = 5), and the response to NMDA (10 to 250 μM) was completely blocked by the addition of Mg^{2+} ions (1 mM, n = 5).

In addition to migration times and pharmacology, the characteristics of the current responses elicited by the separated agonists further confirmed their identities. Spectral analysis of whole-cell current traces of separated components gave power spectra (*16*) that were fitted by the sum of two Lorentzian functions (*17*). From these fits, mean single-channel conductances γ (in picosiemens) and corner frequencies f_{ci} (in hertz) were obtained (Fig. 3); the values of these quantities were in close agreement with the results of earlier studies of rat olfactory and cerebellar neurons (*11*, *18*).

Spectral analysis is helpful in discriminating between different receptor–ion channel complexes in cases where a single ligand activates a single receptor type. When multiple agonists activate the same receptor, however, differentiation between the different agonists cannot be accomplished in general with f_{ci} and γ values alone (*19*). This behavior is illustrated for NMDA- and Glu-evoked receptor responses (Fig. 3, B and D). Without pharmacological intervention, it would be difficult, especially with membrane patches of a high NMDA receptor density, to distinguish between these two agonists with in situ patch-clamp detection. As shown here, this problem can be overcome by using chemical separation before patch-clamp detection, whereby separated components interact with the receptors one at a time. In this way, not only is it possible to separate multiple species in time (Fig. 2, A and C), but it is also possible to analyze whole-cell (Fig. 3) and single-channel (see below) current records.

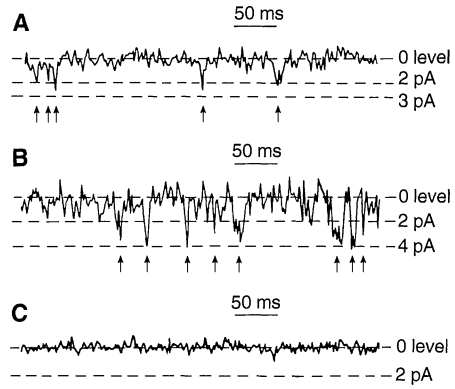

Fig. 4. Single-channel openings elicited by GABA (250 μM) (**A**) and NMDA (10 μM) (**B**) on freshly dissociated rat olfactory interneurons. The background noise trace in (**C**) is from the same recording as (A) before the arrival of the agonist band. The signals from the video tape were low-pass–filtered (250 Hz, −3 dB, 8-pole Bessel filter) and digitized at 500 Hz. Arrows indicate single-channel openings.

Using the outside-out patch-clamp detection configuration, we could resolve single-channel openings for all ligands separated by CE. The low-conductance states were generally ill defined and difficult to distinguish, but the events with the largest amplitudes could be quantitated. GABA-evoked openings were mainly at the 2.0-pA level (Fig. 4A), which corresponds to a mean conductance of 29.1 pS, for a reversal potential of 0 mV. This value is in good agreement with the 24- to 31-pS openings reported for $GABA_A$ receptors in various mammalian central neurons (*18*, *20*). Occasionally, multiple channel openings were seen in GABA-evoked current responses. The main events in NMDA- (Fig. 4B) and Glu-evoked (*21*) NMDA receptor responses yielded an average single-channel current of 3.6 pA; these results correspond to a mean conductance of 52 pS (if we assume a reversal potential of 0 mV) and agree well with the 50-pS channels observed for NMDA receptor–ion channel complexes in earlier studies (*11*, *22*).

Potential applications of this technology include screening orphan receptor ligands, neurotransmitters, and excitotoxins in the extracellular fluid of the mammalian brain. Transfected cells expressing a single receptor clone as a target for different neuroactive modulators could improve the selectivity of these biosensors. Also, neuropeptides that normally operate through metabotropic receptors could be detected with this technique if the receptor clones are expressed together with ion channels that couple to the receptor. For example, G protein–coupled, inwardly rectifying K^+ channels have been functionally expressed for the κ opioid receptor (*23*). Because CE

offers high separation efficiencies (up to $\sim 10^6$ theoretical plates) and can be performed in capillary structures capable of handling sample volumes in the low femtoliter range, the on-line analysis with CE patch-clamp detection of evoked neurotransmitter release from biological microenvironments such as single cells or discrete nerve terminal areas should be feasible because sample integrity is conserved.

REFERENCES AND NOTES

1. L. E. Rabow *et al.*, *Synapse* **21**, 189 (1995).
2. C. E. Jahr and R. A. Lester, *Curr. Opin. Neurobiol.* **2**, 270 (1992).
3. C. J. McBain and M. L. Mayer, *Physiol. Rev.* **74**, 723 (1994).
4. G. A. Rechnitz, T. L. Riechel, R. K. Kobos, M. E. Meyerhoff, *Science* **199**, 440 (1978); R. M. Buch and G. A. Rechnitz, *Anal. Chem.* **61**, 533A (1989); H. M. McConnell *et al.*, *Science* **257**, 1906 (1992); Y. Hu *et al.*, *Brain Res.* **659**, 117 (1994); W. S. Leal *et al.*, *Proc. Natl. Acad. Sci. U.S.A.* **92**, 1033 (1995); *ibid.*, p. 1038.
5. R. I. Hume, L. W. Role, G. D. Fischbach, *Nature* **305**, 632 (1983); S. H. Young and Mu-ming Poo, *ibid.*, p. 634.
6. D. R. Copenhagen and C. E. Jahr, *ibid.* **341**, 536 (1989); T. Maeda *et al.*, *Neuron* **15**, 253 (1995).
7. E. Neher and B. Sakmann, *Nature* **260**, 799 (1976); O. P. Hamill *et al.*, *Pfluegers Arch.* **391**, 85 (1981); B. Sakmann and E. Neher, *Single-Channel Recording* (Plenum, New York, ed. 2, 1995).
8. Even if Glu most likely is the main neurotransmitter acting on NMDA receptors at brain synapses [(2); (24); R. A. Lester and C. E. Jahr, *J. Neurosci.* **12**, 635 (1992)], numerous compounds endogenous to the mammalian brain are known to activate this receptor [(24); X. Li *et al.*, *Neurosci. Lett.* **155**, 42 (1993); P. Q. Trombley and G. L. Westbrook, *J. Neurophysiol.* **64**, 598 (1990)] and to be released by K^+ in a Ca^{2+}-dependent manner [K. Q. Do *et al.*, *J. Neurochem.* **46**, 779 (1986); M. Zollinger *et al.*, *ibid.* **63**, 1133 (1994); M. Kimura *et al.*, *Neuroscience* **66**, 609 (1995)]. Extracellular overflow of NMDA receptor agonists has also been observed during episodes of cerebral ischemia, anoxia, and hypoglycemia [D. W. Choi, *Neuron* **1**, 623 (1988); B. Meldrum, in *Diversity of Interacting Receptors*, L. G. Abood and A. Lajtha, Eds. (New York Academy of Sciences, New York, 1995), vol. 757, pp. 492–505; H. Hagberg *et al.*, *J. Cerebral Blood Flow Metab.* **5**, 413 (1985); M. Sandberg *et al.*, *J. Neurochem.* **47**, 178 (1986); P. Andiné *et al.*, *ibid.* **57**, 230 (1991); O. Orwar *et al.*, *ibid.* **63**, 1371 (1994)]. Furthermore, unnatural NMDA receptor agonists are important for the etiology of some neurodegenerative diseases [J. W. Olney *et al.*, *J. Neuropathol. Exp. Neurol.* **34**, 167 (1975); P. S. Spencer *et al.*, *Science* **237**, 517 (1987); J. H. Weiss and D. W. Choi, *ibid.* **241**, 973 (1988)]. Also, the chemical nature of the coagonist acting on NMDA receptors is not firmly established [S. Cull-Candy, *Curr. Biol.* **5**, 841 (1995)].
9. J. B. Shear *et al.*, *Science* **267**, 74 (1995).
10. H. A. Fishman *et al.*, *Proc. Natl. Acad. Sci. U.S.A.* **92**, 7877 (1995).
11. I. Jacobson, *Neurosci. Res. Commun.* **8**, 11 (1991); _____ and X. Li, *ibid.* **10**, 177 (1992).
12. P. Q. Trombley and G. M. Shepherd, *Curr. Opin. Neurobiol.* **3**, 540 (1993); *J. Neurophysiol.* **71**, 761 (1994).
13. The CE separations were performed in fused-silica capillaries 50 μm in inner diameter (50 cm long) with a high-power supply operated at 12 kV. The inlet end of the capillary was positioned 10 cm above the outlet end. In the sample injections we placed the capillary inlet in sample solution 20 cm above the outlet end for 10 s. The fractured part of the separation capillary was enclosed in a 1-ml polyethylene vial filled with Hepes-saline solution and connected to ground by a Pt wire. We compensated for residual potentials resulting from incomplete grounding by applying a patch-clamp offset potential.
14. Patch pipettes were fabricated from thick-walled borosilicate glass and had tip diameters of ~2 μm (resistance, 5 to 15 megohms; series resistance, <50 megohms). The pipette shanks were treated with Sigmacote (Sigma, St. Louis, MO) and filled with a solution containing 140 mM CsCl, 2 mM $MgCl_2$, 1 mM $CaCl_2$, 11 mM EGTA, and 10 mM Hepes; the pH was adjusted to 7.2 with KOH. Both the outside-out patch-clamp and the whole-cell patch-clamp recording configurations were used, as specified in the text. For outside-out patch-clamp experiments, cells were plated onto cover slips treated with poly-L-lysine and allowed to adhere to the surface for 1 hour before recording. The signals were recorded with a List L/M EPC-7 amplifier, digitized (20 kHz, PCM 2 A/D VCR adapter), and stored on video tape. Data acquisition and initial analysis were performed with programs supplied by J. Dempster, University of Strathclyde, United Kingdom.
15. R. A. Wallingford and A. G. Ewing, *Anal. Chem.* **59**, 1762 (1987).
16. B. Katz and R. Miledi, *J. Physiol. (London)* **224**, 665 (1972); C. R. Anderson and C. F. Stevens, *ibid.* **235**, 655 (1973); D. Colquhoun and A. G. Hawkes, *Proc. R. Soc. London Ser. B* **199**, 231 (1977).
17. The signals from the video tape were low-pass–filtered (1 kHz, −3 dB, 8-pole Butterworth filter) and digitized at 2 kHz. Current records were divided into 0.5-s blocks, and we calculated the power spectra by averaging at least 20 blocks. The resulting spectra were fitted to the sum of two Lorentzian functions:

$$G(f) = \Sigma S(0)_i/[1 + (f/f_{ci})^2]$$

where $G(f)$ is the spectral density, $S(0)_i$ is the low-frequency asymptote of the ith component, f is the frequency, and f_{ci} is the corner frequency (half-amplitude) of the ith component. Curve-fitting was performed with a least squares Levenberg-Marquart algorithm that used proportional weighting. Current traces were used only if the mean current was stable. Apparent single-channel conductances were estimated from

$$\gamma = \sigma^2/[I_m(V - V_{eq})]$$

where σ^2 is the current variance, I_m is the mean current, V is the holding potential (−70 mV), and V_{eq} is the reversal potential (assumed to be 0 mV).
18. M. Kaneda *et al.*, *J. Physiol. (London)* **485**, 419 (1995).
19. P. Ascher, P. Bregestovski, L. Nowak, *ibid.* **399**, 207 (1988).
20. J. Bufler *et al.*, *J. Comp. Physiol. A* **170**, 153 (1992); G. Kilic *et al.*, *Eur. J. Neurosci.* **5**, 65 (1993); B. Schönrock and J. Bormann, *ibid.*, p. 1042.
21. O. Orwar *et al.*, data not shown.
22. C. E. Jahr and C. F. Stevens, *Nature* **325**, 522 (1987); S. G. Cull-Candy and M. M. Usowicz, *ibid.*, p. 525; J. R. Howe *et al.*, *J. Physiol. (London)* **432**, 143 (1991).
23. G. H. Ma *et al.*, *Mol. Pharmacol.* **47**, 1035 (1995).
24. D. K. Patneau and M. L. Mayer, *J. Neurosci.* **10**, 2385 (1990).

25. Helpful discussions with A. Hamberger, M. Sandberg, S. G. Weber, M. E. Meyerhoff, and D. T. Chiu and technical assistance from H. Zhao and R. Dadoo are gratefully acknowledged. This work was supported by grants from the National Institute of Mental Health (MH 45423-06) and the National Institute of Drug Abuse (DA 09873-01). The work of O.O. was supported by the Swedish Natural Science Research Council (K-PD 10481-303), and that of A.M. was supported by the German Gottlieb Daimler- and Karl Benz-Foundation (2.95.32).

1 February 1996; accepted 3 April 1996

Nanoscale Magnetic Domains in Mesoscopic Magnets

Michel Hehn, Kamel Ounadjela,* Jean-Pierre Bucher, Françoise Rousseaux, Dominique Decanini, Bernard Bartenlian, Claude Chappert

The basic magnetic properties of three-dimensional nanostructured materials can be drastically different from those of a continuous film. High-resolution magnetic force microscopy studies of magnetic submicrometer-sized cobalt dots with geometrical dimensions comparable to the width of magnetic domains reveal a variety of intricate domain patterns controlled by the details of the dot geometry. By changing the thickness of the dots, the width of the geometrically constrained magnetic domains can be tuned. Concentric rings and spirals with vortex configurations have been stabilized, with particular incidence in the magnetization reversal process as observed in the ensemble-averaged hysteresis loops.

Mesoscopic magnets are currently being studied for their fundamental and technological properties. These magnets are found in several forms: as particles or patterned submicrometer-sized dots in close interaction with a substrate (*1*–*5*) or as free atomic clusters in beams (*5*, *6*). Very small monodomain Co particles (a few tens of atoms) do not show any hysteretic behavior at room temperature (*6*), whereas in bigger particles, which are relevant to high-density data storage materials, anisotropies build up that lock the magnetic moment in a given direction. Interesting properties are expected as the geometrical dimensions of the particles become comparable to character-

M. Hehn, K. Ounadjela, J.-P. Bucher, Institut de Physique et Chimie des Matériaux de Strasbourg, 23 rue du Loess, 67037 Strasbourg Cedex, France.
F. Rousseaux and D. Decanini, L2M/CNRS, 196 Avenue Henri Ravera, 92225 Bagneux, France.
B. Bartenlian and C. Chappert, Institut d'Electronique Fondamentale, Université Paris-Sud, 91405 Orsay Cedex, France.
*To whom correspondence should be addressed.